Available online at www.sciencedirect.com
SCIENCE DIRECT
International Journal of Heat and Mass Transfer 49 (2006) 4511–4524
International Journal of HEAT and MASS TRANSFER
www.elsevier.com/locate/ijhmt

Experimental and theoretical study of the hot-wire method applied to low-density thermal insulators

R. Coquard [a,*], D. Baillis [b,1], D. Quenard [a]

[a] Centre Scientifique et Technique du Bâtiment (CSTB), 24 rue Joseph FOURIER, 38400 Saint Martin d'Hères, France
[b] Centre Thermique de Lyon (CETHIL), UMR CNRS 5008, Domaine Scientifique de la Doua, INSA de Lyon, Bâtiment Sadi Carnot, 9 rue de la physique, 69621 Villeurbanne Cedex, France

Received 4 October 2005; received in revised form 2 May 2006
Available online 12 July 2006

Abstract

The use of the hot wire method for thermal conductivity measurement has recently known a significant increase. However, this method is theoretically not applicable to materials where radiative heat transfer is not negligible such as low-density thermal insulators. In order to better understand the influence of radiative contribution, we developed a two dimensional simulation of transient coupled heat transfer and made hot-wire measurements on low-density Expanded PolyStyrene (EPS) foams. The analysis of theoretical and experimental results shows that classical hot-wire apparatus are poorly adapted to low-density insulators. However, if an appropriate hot-wire apparatus is used, the estimated equivalent thermal conductivity is in close agreement with that estimated by the guarded hot-plate method.

Keywords: Hot-wire; Heat transfer; Radiation/conduction coupling; Equivalent thermal conductivity; Edge effects

1. Introduction

The accuracy of thermal properties measurement takes on particular importance in numerous physical, chemical or medical applications given that it has a direct influence on the estimation of heat losses, or temperature rise. For purely conductive materials, the basic energy equation and the Fourier conduction law govern heat transfer which depends on two parameters: the thermal conductivity and the specific heat. Standards measuring methods for these parameters are based on steady state techniques. For the thermal conductivity, the principle of the standard guarded hot plate method is to measure the heat flux passing through a slab of materials subjected to a one dimensional steady state heat transfer. This technique gives very accurate results. Nevertheless, it is restricting given that the slab must have large and standard dimensions and that it requires especially long measuring durations.

That is the reason why, during the last two decades, there has been a significant development of the transient methods of measurement of thermophysical properties on a broad range of materials. As example, Lazard et al. [1] studied the application of the flash method to the measurement of the intrinsic diffusivity of semi-transparent media in which radiative heat transfer is significant. They proposed a complete methodology to adapt the method to this kind of materials. Nevertheless, the transient method which is the most widely used for the measurement of thermal conductivity is the so-called hot-wire method. Indeed, it is relatively simple and fast as it is based on the transient measurement of the temperature rise of a uniformly heated wire. Moreover, the measurement could be made on samples with any shapes and relatively small sizes. It has been used in numerous studies dealing with solid and pasty thermal insulators [2] or soil [3] and gives satisfactory results.

* Corresponding author. Tel.: +33 (0)4 76 76 25 53.
E-mail addresses: r.coquard@cstb.fr (R. Coquard), dominique.baillis@insa-lyon.fr (D. Baillis).
1 Tel.: +33 (0)4 72 43 84 74.

0017-9310/$ - see front matter
doi:10.1016/j.ijheatmasstransfer.2006.05.016

Nomenclature

a	thermal diffusivity (m^2/s)
C_p	specific heat of the porous medium (J/kg/K)
C_w	specific heat of the material constituting the hot-wire
$I(r, z, \theta, \varphi)$	radiant intensity at point (r, z) in the direction (θ, φ) (W/m^2)
k	thermal conductivity (W/m/K)
L	length of the wire (m)
$P((\theta', \varphi'), (\theta, \varphi))$	global phase function for the scattering from direction (θ', φ') to direction (θ, φ)
q	heat flux (W/m^2)
$\dot{Q}$	heating power per unit length (W/m)
r	radial coordinate
R	radius (m)
t	heating time (s)
T	temperature (K)
TR_c	thermal contact resistance (m^2 K/W)
z	axial coordinate

Greek symbols

β, κ and σ	global extinction, absorption and scattering coefficients (m^{-1}) ($\beta = \kappa + \sigma$)
σ_{SB}	Stefan–Boltzmann constant ($\approx 5.67 \times 10^{-8}$ $W/m^2/K^4$)
ε_w	emissivity of the wire
λ	Wavelength of radiation (μm)
ρ_c	density of the foam (kg/m^3)
ρ_w	density of the material constituting the hot-wire (kg/m^3)
(θ, φ)	direction angles of the radiant intensity
ϕ	radial angle
$\omega = \sigma/\beta$	scattering albedo
Ω_w	electrical resistance of the wire (Ω)
Ω	solid angle

Subscripts

c	conductive
init	initial
max	maximal coordinate
r	radiative
ROSS	from Rosseland approximation
w	of the wire

Superscripts

r	along the radial coordinate
z	along the axial coordinate

However, as the method is based on the Fourier diffusion law, it is theoretically not applicable to materials where radiative heat transfer occurs and then, it is restricted to opaque or ideally transparent materials.

Several authors [4–6] tried to extend the method to nearly transparent media in order to measure the thermal conductivity of liquids using the hot-wire apparatus.

Other studies [7,8] have also been conducted in order to apply the classical hot-wire method to semi-transparent media in which the total heat flux is the result of the coupled conduction–radiation heat transfer. Their aim was to determine whether the method could be used to estimate their "equivalent" conductivity. This property corresponds to the conductivity of the purely conductive material that would lead to the same total heat flux under the same thermal boundary conditions. It is generally measured by the non-convenient guarded hot-plate method. Ebert and Fricke [7] have been interested in the influence of radiative transport on hot-wire measurement in semi-transparent media. They modelled the transient combined conductive and radiative heat transfer by solving the one-dimensional axisymmetric energy equation and radiation problem using the method of successive approximation and the Milne-Eddington approximation respectively. This latter is rigorously only applicable for optically thick media. They also neglected the radiative energy emitted by the wire surface. The theoretical results permit them to conclude that there is a lower limit of the extinction coefficient of the medium above which the radiative transfer could be treated using a diffusion model. When the extinction coefficient exceeds this limit, the equivalent thermal conductivity of the material could be determined by the classical hot-wire method. In a recent study, Gross and Tran [8] have simulated more rigorously the hot-wire measuring method by modelling the transient coupled heat transfer in a grey semi-transparent porous medium bounded by two infinite coaxial cylinders. They solved numerically the energy equation and radiative transfer equation (RTE) using the control volume method and the discrete ordinates method respectively. They studied the influence of the extinction coefficient, emissivity of the wire and the heating power and showed that the hot-wire method works accurately only in cases where the extinction coefficient exceeds a minimum value which increases with the temperature. This remark is in close agreement with the conclusion of Ebert and Fricke [7]. They also brought up the problem of the reference temperature for the measured thermal conductivity given that the temperature of the wire increases during the measurement. However, the study was only theoretical and concerned ideal absorbing and scattering grey media whose radiative and conductive properties are not related to that of real semi-transparent materials.

In this work, we present a theoretical and experimental study of the hot-wire measurement method applied to low-density EPS foams for which it leads to noticeable differences with the results of the standard guarded hot plate method. The aim is to analyze the influence of the radiative contribution on the estimated equivalent thermal conductivity and to propose, if possible, an extension of the classical hot-wire technique to this kind of porous materials. At first, we recall the principle of the standard method. Then, we describe the theoretical model developed to take into account the influence, on the temperature rise of the wire, of the disturbing phenomenon such as the radiative contribution, the thermal inertia of the wire, the edge effects or the thermal contact resistance between the wire and the medium. The 2-D axisymmetric energy equation and Radiative Transfer Equation are solved numerically. The radiative and conductive properties of the EPS foams used have been determined in a previous study [9]. The analysis of theoretical results permits us to explain the noticeable differences between the thermal conductivity measured by the classical hot-wire method and those measured by the guarded hot-plate method.

2. Governing equations

2.1. Infinite wire in a purely conductive medium

The principle of the standard transient hot-wire method is to heat a thin and long wire immersed in the sample in order to generate a transient temperature field in the material. The measurement of the temperature rise near the wire permits to determine the heat conductivity of the porous medium. Indeed, heat balance is governed by the energy equation detailed in [10]. If we assume that the medium is at a uniform temperature before the beginning of the heating, that there is no thermal contact resistance between the wire and the medium and that the wire is infinitely long and has negligible thermal inertia, the solution of the energy equation for a purely conductive medium leads to:

$$\Delta T_{\text{wire}} = \frac{\dot{Q}}{4\pi \cdot k_c} Ln\left(\frac{4 \cdot a \cdot t}{R_{\text{wire}}^2 \cdot C}\right) \quad \text{when} \quad \frac{R_w^2}{4 \cdot a \cdot t} \ll 1 \tag{1}$$

where a (m^2/s) is the thermal diffusivity of the material $\left(a = \frac{k_c}{\rho \cdot C_p}\right)$, C is a constant: $C = e^\gamma \approx 1.781$ and γ the Euler's constant.

The temperature of the material near the wire also follows a similar evolution with the time t. This formula shows that it is sufficient to know the temperature T_1 and T_2 measured at time t_1 and t_2 near the wire to determine the thermal conductivity k_c of the material. Indeed, we have:

$$k_c = \frac{\dot{Q}}{4\pi} \frac{Ln(t_2) - Ln(t_1)}{T_2 - T_1} \tag{2}$$

Measurements on solid materials are generally made using a wire of approximately 250 μm in diameter and require relatively long measuring duration (typically several hundred of seconds).

2.2. Finite wire in a semi-transparent medium

In practice, the inertia of the wire is not negligible, the contact between the wire and the surrounding medium is not perfect and its length L is limited. In the case of usual opaque materials, edge effects can be neglected. However, we will see that it is important to study the influence of these effects in the case of semi-transparent low-density materials. In order to model the edge effects, the axisymmetric temperature distribution in the medium must be a function of the radius r, the time t and the z coordinate along the wire (see Fig. 1).

2.2.1. Energy equation

The heat balance in a semi-transparent, conductive but non convective medium is still governed by the energy equation which, now, has to take into account the radiative heat transfer:

$$\rho \cdot C_p \cdot \frac{\partial T}{\partial t} = -\nabla(\vec{q}_t) = -(\nabla(\vec{q}_r) + \nabla(\vec{q}_c)) \tag{3}$$

In the case of an axisymmetric heat transfer in a homogeneous and isotropic medium, the temperature field is independent of the polar angle ϕ [10]. If we also assume that the variations $\frac{\partial k_c}{\partial r}$ and $\frac{\partial k_c}{\partial z}$ are negligible, we finally have:

$$\nabla(\vec{q}_c) = -k_c \cdot \frac{\partial^2 T}{\partial r^2} - \frac{1}{r} \cdot k_c \cdot \frac{\partial T}{\partial r} - k_c \frac{\partial^2 T}{\partial z^2} \tag{4}$$

In the previous equation, the thermal conductivity k_c depends on the temperature of the material. Nevertheless, for clarity purpose, we will omit to specify it afterwards.

2.2.2. Radiative transfer equation

Regarding the radiative heat transfer, the radiative flux is related to the intensity field in the medium:

$$\vec{q}_r = q_r^r \cdot \vec{e}_r + q_r^z \cdot \vec{e}_z$$

with

$$q_r^r(r,z) = \int_{\Omega=4\pi} I(r,z,\theta,\varphi) \cdot \mu \, d\Omega,$$
$$q_r^z(r,z) = \int_{\Omega=4\pi} I(r,z,\theta,\varphi) \cdot \xi \, d\Omega \tag{5}$$

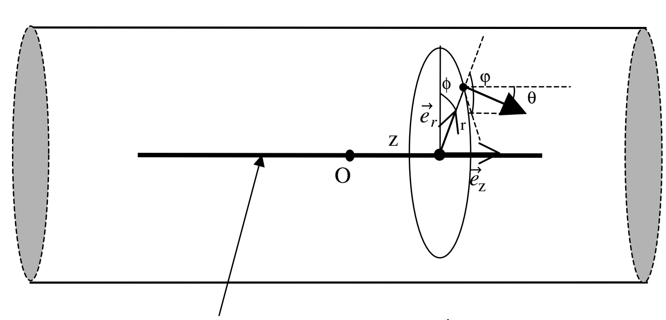

Fig. 1. Illustration of the cylindrical coordinates system around the wire.

and

$$\nabla(\vec{q}_r) = \frac{1}{r}\cdot\frac{\partial}{\partial r}(r\cdot q_r^r) + \frac{\partial q_r^z}{\partial z} \tag{6}$$

The radiation intensity field is governed by the Radiative Transfer Equation (RTE) described in details in [11]. The RTE takes into account the emission, the absorption and the scattering of the radiation by the participating medium. For a 2-D axisymmetric radiative transfer in a isotropic material with azimuthal symmetry, this equation is

$$\begin{aligned}&\frac{\mu}{r}\cdot\frac{\partial(r\cdot I(r,z,\theta,\varphi))}{\partial r} - \frac{1}{r}\cdot\frac{\partial(\eta\cdot I(r,z,\theta,\varphi))}{\partial\phi} + \xi\cdot\frac{\partial I(r,z,\theta,\varphi)}{\partial z}\\ &\quad + \beta\cdot I(r,z,\theta,\varphi)\\ &\quad = \kappa_\lambda I^0(T) + \frac{\sigma}{4\pi}\int_{\Omega'=4\pi} P(v)\cdot I(r,z,\theta',\varphi')\,\mathrm{d}\Omega'\end{aligned} \tag{7}$$

where $\eta = \sin\theta\cdot\sin\varphi$; $\mu = \sin\theta\cdot\cos\varphi$ and $\xi = \cos\theta$ are the directing cosines and $v = \mu\cdot\mu' + \eta\cdot\eta' + \xi\cdot\xi'$ is the cosine of the angle between incident and scattering direction.

We can notice that it is necessary to know the temperature field in the medium to solve the RTE and to determine the radiation intensity field.

2.2.3. Radiative boundary conditions

At the periphery of the wire ($r = R_\mathrm{w}$), the boundary conditions of the RTE for an emissive and diffusely reflecting wire are

$$\begin{aligned}&I(R_\mathrm{w},z,\theta,\varphi)\\ &\quad = \varepsilon_\mathrm{w}\cdot I^0(T_\mathrm{w}) + \frac{1-\varepsilon_\mathrm{w}}{\pi}\cdot\int_{\Omega=2\pi;\mu'<0} I(R_\mathrm{w},z,\theta',\varphi')\cdot|\mu'|\,\mathrm{d}\Omega'\\ &\qquad \text{for } \mu>0 \text{ and } -L/2<z<L/2\end{aligned} \tag{8}$$

At the tips of the wire ($z = \pm L/2$ and $r < R_\mathrm{w}$), there are similar boundary conditions.

We also have the following relations for the radiative intensities far from the wire:

$$\begin{aligned}&I(r\to\infty,z,\theta,\varphi) = I^0(T_\mathrm{init}) \quad \text{for } \mu<0\\ &I(r,z\to+\infty,\theta,\varphi) = I^0(T_\mathrm{init}) \quad \text{for } \xi<0 \text{ and}\\ &I(r,z\to-\infty,\theta,\varphi) = I^0(T_\mathrm{init}) \quad \text{for } \xi>0\end{aligned} \tag{9}$$

2.2.4. Thermal boundary conditions

Given that the inertia of the wire and the radiative contribution are no more negligible and that the length of the wire is not infinite, the thermal boundary condition around the wire is also modified to take into account the energy necessary to heat the wire, the axial conductive heat flux and the radiative flux emitted by the wire. We then have:

$$\begin{aligned}&\rho_\mathrm{w}\cdot C_\mathrm{w}\cdot\pi R_\mathrm{w}^2\cdot\Delta z\cdot\frac{\mathrm{d}T_\mathrm{w}}{\mathrm{d}t}\\ &\quad = \dot{Q} - q_r^{r=R_\mathrm{w}}\cdot 2\pi\cdot R_\mathrm{w}\cdot\Delta z + \pi\cdot R_\mathrm{w}^2\cdot k_\mathrm{w}\cdot\left(\frac{\mathrm{d}T_\mathrm{w}}{\mathrm{d}z}\right)_{z=\Delta z/2}\\ &\qquad - \pi\cdot R_\mathrm{w}^2\cdot k_\mathrm{w}\left(\frac{\mathrm{d}T_\mathrm{w}}{\mathrm{d}z}\right)_{z=-\Delta z/2} + 2\pi\cdot R_\mathrm{w}\cdot\Delta z\cdot k_\mathrm{c}\cdot\left(\frac{\mathrm{d}T}{\mathrm{d}r}\right)_{r=R_\mathrm{w}}\end{aligned} \tag{10}$$

where Δz is the length of the wire element considered.

Moreover, we have seen that the thermal contact between the wire and the porous medium is not perfect, and then, we must introduce a thermal contact resistance $\mathrm{TR_c}$ at the interface wire/medium. This contact resistance acts on the heat transferred by conduction from the wire to the surrounding medium and modifies the last term on the right hand side of Eq. (10). In our model, we take into account this thermal resistance by calculating a global thermal resistance $\mathrm{TR_{tot}}$ that is the sum of the contact resistance and the resistance due to conduction.

At the tips of the wire, the previous equation is modified to take into account the radiative and conductive heat transfer between the tip of the wire and the surrounding medium.

As regards the boundary conditions, the medium is still at a uniform temperature before the beginning of the heating, and the temperature far from the wire is not affected by the heating:

$$\forall r \text{ and } z,\; T(r,z,0) = T_\mathrm{init};\; \lim_{z\to\pm\infty} T(r,z,t) = T_\mathrm{init}$$

and

$$\lim_{r\to\infty} T(r,z,t) = T_\mathrm{init} \tag{11}$$

3. Numerical resolution of the transient coupled heat transfer

In order to solve the energy equation (3) and to calculate numerically the variation of the temperature field during the transient heat transfer, we use an explicit time marching technique. As it is necessary to know the temperature field to solve the RTE and to compute $\nabla\vec{q}_r$, an internal iterative process should be performed at each time step to produce consistency between the temperature profile and the radiation field. However, when the time interval between two time steps is small ($\Delta t < 0.1$ s in our study), this internal iterative process is superfluous and the temperature field at the new time step could be calculated directly using the radiation intensity field at the previous time step without causing errors. In their study on the temperature rise of a cylindrical glass gob, Viskanta and Lim [12] use the same simplification.

3.1. Resolution of the energy equation and computation of the temperature field

At each time step, the resolution of the energy equation permits to compute the new temperature distribution from the temperature and radiation intensity profiles at the previous time step. To solve this equation we use a spatial discretization dividing the volume in $nR \times nZ$ elementary volume. In order to limit the computation time and memory requirement, the heat transfer problem is solved in a finite volume around the wire. Then the calculations are restricted to $R_w < r < R_{max}$ and $-z_{max}/2 < z < z_{max}/2$. This volume must be sufficiently important in order for the theoretical temperature profile near the wire, not to be influenced by the value of R_{max} and z_{max}. At the centre and on the radial faces of each elementary volume, there is a node. The numerical resolution computes the temperature at the centre (noted $T_{i,j}$) and on the boundary (noted $T_{i\pm1/2,j}$) of each volume. The discretization along the z-axis is uniform: $\Delta z = \frac{z_{max}}{nZ}$, whereas the discretization of the radius provides narrower volumes near the wire where important temperature gradients are found:

$$\Delta r_{i+1} = 1.8 \times \Delta r_i \quad \text{for } i = 1, nR \text{ and } \sum_{i=1}^{nR} \Delta r_i = (R_{max} - R_w) \tag{12}$$

The temperature $T_{0,j}$ of the volumes $(0,j)$ for which $j_{lim1} < j < j_{lim2}$ correspond to the temperature of the wire noted $T_{w,j}$ and is assumed uniform as the conductivity of the wire is very important compared to that of the porous medium: $T_{0,j} = T_{1/2,,j} = T_{w,j}$.

For the nodes (i,j) containing the semi-transparent medium, if we express the energy equation (3) in a discretised form using Eq. (4), we could express the new temperature from the temperature profile and radiative divergence at previous time step:

$$\begin{aligned} T_{i,j}^{t+1} = T_{i,j}^{t} + \frac{\Delta t}{\rho \cdot C_p} \cdot \Bigg[& 4 \cdot k_c \frac{T_{i+1/2,j}^{t} - 2 \cdot T_{i,j}^{t} + T_{i-1/2,j}^{t}}{\Delta r_i^2} \\ & + \frac{k_c}{r_i} \cdot \left(\frac{T_{i+1/2,j}^{t} - T_{i-1/2,j}^{t}}{\Delta r_i} \right) \\ & + k_c \cdot \frac{T_{i,j+1}^{t} - 2 \cdot T_{i,j}^{t} + T_{i,j-1}^{t}}{\Delta z_j^2} - \nabla(\vec{q}_r)_{i,j}^{t} \Bigg] \end{aligned} \tag{13}$$

where $\nabla(\vec{q}_r)_{i,j}^{t}$ is the divergence of the radiative heat flux at the node i,j at time step t.

Similar relations could be found easily for the nodes placed on the boundary of the elementary volumes and for the wire nodes by discretising Eqs. (3), and (10). For the nodes $(1,j)$ placed near the wire (for which $-L/2 < z_{1,j} < L/2 \Longleftrightarrow j_{lim1} < j < j_{lim2}$), we must apply a energy balance to express the temperature at the new time step. This energy balance must take into account the possible contact resistance between the wire and the surrounding medium.

Finally, the thermal boundary conditions far from the wire (Eq. (11)) in a discretised form are

$$T_{nR,j}^{t} = T_{init} \quad \forall j \text{ and } t; \quad T_{i,0}^{t} = T_{init} \quad \forall i \text{ and } t$$

and

$$T_{i,nz+1}^{t} = T_{init} \quad \forall i \text{ and } t \tag{14}$$

3.2. Resolution of the 2-D axisymmetric RTE using the discrete ordinates method

In order to calculate the radiative flux $(\vec{q}_r)_{i,j}$ and the radiative flux divergence $\nabla(\vec{q}_r)_{i,j}$ in each point of the spatial discretization, it is necessary to solve the 2-D axisymmetric Radiative Transfer Equation (Eq. (11)). Several numerical methods can be used to solve the RTE (spherical harmonics method, the zone method of HOTTEL, the ray-tracing methods ...). In our study, we use the Discrete Ordinates Method based on a spatial discretization of the area around the wire and on an angular discretization of the space. The angular discretization allows replacing the angular integrals by finite summations over n_d discrete directions m (μ_m, η_m, ξ_m) with given weighting factors w_m. The spatial discretization must be the same as the one used for the numerical resolution of the energy equation. The 2-D discrete ordinates solution for a radiatively participating medium in a cylindrical enclosure has been widely described, notably by Carlson and Lathrop [13] or Jendoubi et al. [14] and we will not detail it in this article.

Once the discretised intensity field in the semi-transparent medium around the wire has been determined, the radiative flux and radiative flux divergence are calculated using the discretised form of Eqs. (9) and (10):

$$(q_r^r)_{i,j} = \left[\sum_{m=1}^{nd} I_{i,j}^m \cdot \mu_m \cdot w_m \right] \quad \text{and} \quad (q_r^z)_{i,j} = \left[\sum_{m=1}^{nd} I_{i,j}^m \cdot \xi_m \cdot w_m \right], \tag{15}$$

$$\begin{aligned} \nabla(\vec{q}_r)_{i,j} = & \frac{1}{r_i} \cdot \frac{r_{i+1/2} \cdot (q_r^r)_{i+1/2,j} - r_{i-1/2} \cdot (q_r^r)_{i-1/2,j}}{\Delta r_i} \\ & + \frac{(q_r^z)_{i,j+1/2} - (q_r^z)_{i,j-1/2}}{\Delta z}. \end{aligned} \tag{16}$$

3.3. Validation of the numerical method

The numerical resolution of the 2-D axisymmetric radiative problem has been tested by comparing the results of our model with published results [14,15] for different media where only radiative transfer occurs. The accuracy of the numerical method is strongly dependent on the quadrature used for the angular discretization. We have tested different S_N quadratures. The results obtained when using the quadrature points and weights of the S_6 scheme prove to be quiet satisfactory in all cases and we will use this quadrature in all the following theoretical calculations.

Concerning the entire 2-D transient radiation/conduction coupling problem, no previous results has already been published. The previous published results only studied 1-D transient heat transfer [7,8]. Thus, we check the validity of our numerical resolution by carrying out the computations for two limiting cases:

- Purely conductive medium ($\beta \to \infty$, $k_c = 0.035$ W/m/K) surrounding an infinite wire ($L \to \infty$) with negligible inertia ($\rho_w \cdot C_w \cdot \pi \cdot R_w^2 \to 0$).

- Transparent medium ($\beta = 0$; $k_c = 0.035$ W/m/K) surrounding an infinite wire ($L \to \infty$) with negligible inertia ($\rho_w \cdot C_w \cdot \pi \cdot R_w^2 \to 0$).

The first test case corresponds to the ideal case described in Section 2.1 and the analytical solution is given by Eq. (1) when the condition $\frac{R_w^2}{4 \cdot a \cdot t} \ll 1$ is satisfied. In order to compare the numerical solution with the analytical one, we have carried out calculations fixing β to a very large value ($\beta = 10^6$ m^{-1}) corresponding to a nearly opaque material. The other parameter used for the numerical resolution are $\rho_w \cdot C_w = 4720$ J/m^3/K, $k_w = 100$ W/m/K, $\rho \cdot C_p = 36000$ J/m^3/K, $R_w = 0.0002$ m, $\dot{Q} = 1.033$ W/m, $T_{init} = 296$ K, $nR = 12$ and nZ=30. Calculations were carried out by setting $R_{max} = 0.15$ m, $z_{max} = 2$ m and $L = 1$ m. We have checked that these values of R_{max}, z_{max} and L are sufficiently important in order for the theoretical results to remain independent of their values. The results obtained then correspond to those of an infinite medium surrounding an infinite wire.

When comparing analytical and numerical results, we noticed that the temperature rise calculated numerically by setting $\beta = 10^6$ is very close to the analytical solution as the relative differences is always lower than 0.5% when $t > 5$ s and lower than 0.1% when $t > 30$ s. The maximum difference between analytical and numerical results is found for the very low values of time t. This can be explained by the fact that the inertia effects, which are significant at the beginning of the heating, are neglected by the analytical solution whereas the numerical solutions take into account a low inertia of the wire. Then, the numerical simulation proves to be very accurate when the spatial discretization $nR = 12$, $nZ = 30$ and the S6 angular quadrature are used.

Regarding the second test case, it corresponds to the transparency limit $\beta = 0$. Under this assumption, the conductive and radiative contributions can be evaluated separately as the surrounding medium does not participate to the radiative transfer ($(\nabla\vec{q}_r)_{i,j}^t = 0$). The radiative heat flux emitted by the wire only depends on the emissivity of the wire and its local temperature. It can be evaluated by the following analytical relation:

$$(q_r^r)_{1/2,j} = \varepsilon_w \cdot \sigma_{SB} \cdot (T_{w,j}^{t4} - T_{init}^4) \quad \text{for } j_{lim1} < j < j_{lim2}$$
$$(q_r^z)_{0,j\,lim\,1+1/2} = \varepsilon_w \cdot \sigma_{SB} \cdot (T_{w,j}^{t4} - T_{init}^4)$$
$$(q_r^z)_{j\,lim\,2-1/2} = \varepsilon_w \cdot \sigma_{SB} \cdot (T_{w,j}^{t4} - T_{init}^4)$$

The numerical results obtained by setting $(\nabla\vec{q}_r)_{i,j}^t = 0$ and using the previous boundary conditions in the purely conductive problem have been compared to those obtained by setting $\beta = 10^{-6}$ m^{-1} in the coupled conduction–radiation problem. The deviation between the two numerical method is always lower than 0.001 in the time range 10–600 s. Thus, the numerical resolution of the radiative problem proves to give satisfactory results.

As a conclusion the calculations carried out for the two limiting cases show that, when using the spatial discretisation $nR = 12$, $nZ = 30$ and the S6 quadrature, our numerical method accurately simulate the temperature rise near the hot wire.

4. Results and discussion

In order to analyse the influence of the radiative transfer on the hot-wire method applied to low-density thermal insulators, we made a series of experimental measurements on four low-density EPS foams using the different hot wire measuring systems. The results have been compared to theoretical predictions. We used the experimental and theoretical temperature rise to analyse the evolution of the thermal conductivity k_{hot} estimated in classical hot-wire measuring method by Eq. (2) for purely conductive media.

$$k_{hot} = \frac{\dot{Q}}{4\pi} \frac{Ln(t_2) - Ln(t_1)}{T_2 - T_1} \tag{17}$$

For experimental results, in order to limit the fluctuations, the value of k_{hot} at time t has been evaluated from the temperature at time $t_1 = t - 36$ s and $t_2 = t + 36$ s. Whereas, for theoretical results, we used $t_1 = t - 2$ s and $t_2 = t + 2$ s. An analysis of the influence of the different parameters has also been conducted.

4.1. Description of the low-density thermal insulators studied

Measurements have been made on four different EPS foams in which we show (in Ref. [9]) that the radiative heat transfer constitutes a significant part of the total heat transfer. Their equivalent thermal conductivities $k_{eq.m}$ have been measured by the guarded hot-plate method for an average temperature of 296 K. These equivalent conductivities can be taken as references. The global radiative properties (β, ω and $P(\nu)$) as well as the conductive properties (k_c) of the foams, required for the numerical simulation, have been determined in our previous study [9]. Thus, we could compute the theoretical equivalent thermal conductivity $k_{eq.th}$ from the radiative and conductive properties by solving numerically the steady-state one-dimensional coupled heat transfer using the discrete ordinates method in Cartesian coordinates and the control volume method. Given that the radiative contribution is relatively important in the EPS foams studied, their theoretical equivalent conductivity varies with the boundary conditions and especially with the average temperature of the material. For the temperature range 296–320 K, the variations of $k_{eq.th}$ for the four EPS foams have been proved to follow the law:

$$k_{eq\cdot th} = b_1 \cdot T^2 + b_2 \cdot T + b_3 \tag{18}$$

where b_1 (W/m/K^3), b_2 (W/m/K^2) and b_3 (W/m/K) are constants peculiar to each foam.

All the characteristics of the four EPS foams are regrouped in Table 1. Regarding the sample number 4, we checked that it is sufficiently dense to be considered as an optically thick medium contrary to the other lighter samples. For this sample, the radiative heat transfer problem is then treated using the Rosseland approximation.

Table 1
Thermal characteristics of the four low-density EPS foams used

Sample number	ρ (kg/m^3)	$k_{eq.m}$ (W/m/K) at 296 K	β (m^{-1})	ω	g	b_1 (W/m/K^3), b_2 (W/m/K^2), b_3 (W/m/K)	$k_{eq.th}$ (W/m/K) at 296 K
1	10	0.0482	608.2	0.905	0.58	$b_1 = 8.878 \times 10^{-7}$, $b_2 = -2.09 \times 10^{-4}$, $b_3 = 0.0344$	0.05003
2	12.6	0.0428	763.9	0.901	0.58	$b_1 = 7.606 \times 10^{-7}$, $b_2 = -1.808 \times 10^{-4}$, $b_3 = 0.0328$	0.04554
3	18.3	0.0396	1072.4	0.889	0.6	$b_1 = 5.308 \times 10^{-7}$, $b_2 = -9.081 \times 10^{-5}$, $b_3 = 0.02189$	0.04136
4	32.0	0.03395	$\beta_{ROSS} = 1400$	–	–	$b_1 = 2.636 \times 10^{-7}$, $b_2 = -2.46 \times 10^{-5}$, $b_3 = 0.01803$	0.03395

This approximation allows to directly relate the radiative flux to the temperature gradient and greatly simplifies the resolution:

$$q_r^r = -\frac{16 \cdot \sigma_{SB}}{3 \cdot \beta_{ROSS}} T^3 . \frac{\partial T}{\partial r} = k_{ROSS} \cdot \frac{\partial T}{\partial r}$$
$$q_r^z = -\frac{16 \cdot \sigma_{SB}}{3 \cdot \beta_{ROSS}} T^3 \cdot \frac{\partial T}{\partial z} = k_{ROSS} \cdot \frac{\partial T}{\partial z} \tag{19}$$

4.2. Description of the hot-wire apparatus

The hot-wire measuring system used is composed of different apparatus (see Fig. 2): the measuring apparatus including the heated wire and two thermocouples placed near the wire, an intensity generator supplying the hot-wire and an acquisition system connected to the thermocouples allowing to record the temperature rise.

The thermocouples are placed at a distance of approximately 1 mm from the centre of the heated wire. In order to ascertain that the thermocouples are well-positioned, the three elements are embedded in a slab of kapton of 220 μm in thickness (see Fig. 2). To avoid colder bridge, the kapton slab between the wire and the thermocouples is cut.

We used three different apparatus which differ, among other, by their length L (wire 1: $L = 0.2$ m; wire 2: 0.1 m or wire 3: 0.05 m). Wire 2 and wire 3 are usually used for measurements on opaque materials whereas wire 1 has been especially made for this study. Actually, the heated wires are constituted of a curved wire of constantan of parallelogram cross section ($500 \times 220\ \mu m^2$ for wire with $L = 0.2$ m) between which a slab of kapton is placed (see Fig. 2). We could notice that the wires have actually not a circular cross sections and that the heat is not generated homogeneously as the Joule effect only occurs in the constantan element. However, owing to the very small size of the wire, we will assume that the generated heat transfer remains axisymmetric and that the heat is homogeneously dissipated in the wire. In order to take into account as faithfully as possible the inertia of the wires, the fictitious circular cross sections of the wires are equal to the real cross sections of the whole kapton + constantan. Moreover, the thermophysical properties of the wires ($\rho_w \cdot C_w$) and k_w are assumed homogeneous and are calculated by averaging the properties of the two components (kapton and constantan). The properties of all the wires are regrouped in Table 2.

Regarding the emissivity of the wires, it is difficult to determine it precisely. However, in order to estimate it,

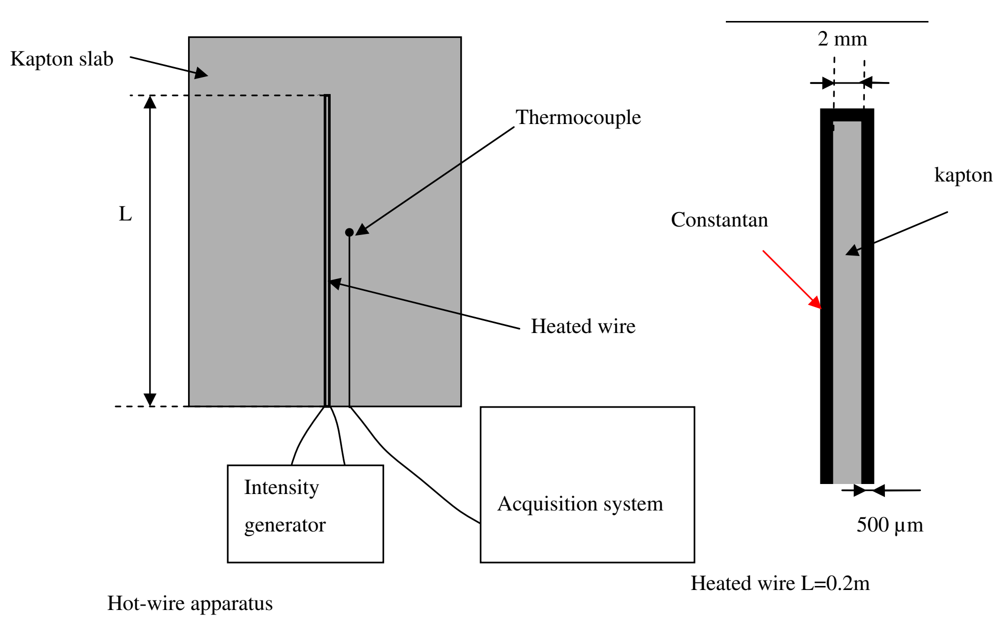

Fig. 2. Illustration of the structure of the hot-wire apparatus and the heated wire.

Table 2
Physical and thermophysical characteristics of the different hot-wire used

	L (m)	R_w (μm)	$\rho_w \cdot C_w$ (J/m^3/K)	k_w (W/m/K)
Wire 1	0.2	460	2.44×10^6	7
Wire 2	0.1	200	3.32×10^6	13
Wire 3	0.05	200	3.32×10^6	13

we made transmittance and reflectance measurements on thin slabs (≈200 μm) of kapton and reflectance measurements on sheets of constantan using an FTIR spectrometer. The experimental results show that a slab of kapton of 200 μm thick could be considered as opaque and purely absorbing and that the constantan has a very low reflectivity in the Medium Infrared Radiation range ($2\ \mu m < \lambda < 25\ \mu m$). As a consequence, we will assume that the wire is perfectly emissive: $\varepsilon_w = 1$.

The heat dissipated in the wire by Joule effect is proportional to the electrical resistance $\Omega_w(\Omega)$ of the wire and the heating power per unit length is then

$$\dot{Q} = \frac{W}{L} = \frac{\Omega_w \cdot i^2}{L} \tag{20}$$

These resistances have been measured using a multimeter and are respectively 16.25, 21 Ω and 7.75 Ω for the wire with $L = 0.2$ m, $L = 0.1$ m and $L = 0.05$ m.

4.3. Comparison of experimental and theoretical results

We used the different hot-wire apparatus with various lengths (wire 1–2 and 3) to measure the temperature rise for each of the EPS foam samples presented. Measurements were made for the time range 1–600 s using the thermocouple distant of approximately 1 mm from the wire and different heating power $\dot{Q}$. The measurements are made by placing the hot-wire apparatus between two slabs of the foam sample considered. In order to ensure a good thermal contact between the hot-wire and the sample, the two slab are slightly compressed using a heavy object. The dimensions of the foam slabs used are sufficiently important to consider that the porous medium surrounding the heated-wire is infinite.

We also carried out the corresponding theoretical calculation for each EPS foams samples using the conductive and radiative properties and the foam densities illustrated in Table 1 and the properties of the wires presented in Section 4.2. The other parameters necessary for the numerical resolution are

$$T_{\text{init}} = 296\ \text{K}; \quad C_p = \frac{(\rho - \rho_{\text{air}}) \cdot C_{\text{PS}} + \rho_{\text{air}} \cdot C_{\text{air}}}{\rho}$$

with $C_{\text{air}} = 1006$J/kg/K and $C_{\text{PS}} = 1200$ J/kg/K.

When calculations are made for wires 1 or 2, the numerical parameters used are $nR = 12$; $nZ = 30$; S_6 quadrature; $Z_{\max} = 0.3$ m and $R_{\max} = 0.15$ m whereas we used $nR = 12$; $nZ = 60$; S_6 quadrature; $Z_{\max} = 0.3$ m and $R_{\max} = 0.15$ m for the simulations concerning wire 3. The values of $R_{\max}$ and $Z_{\max}$ have been chosen in order for the theoretical results to remain independent of their values. The results obtained then correspond to those of an infinite medium surrounding a finite wire with varying length L. Finally, the theoretical calculations for an infinitely long wire ($L \to \infty$) have actually been carried out by setting $L = Z_{\max} = 10$ m.

A preliminary study in which we varied the theoretical contact resistance R_c at the interface plane/medium have shown that it has almost no influence on the measurement as long as it is lower than 0.01 m^2 K/W whereas a bad thermal contact ($R_c > 0.01$ m^2 K/W) could cause significant errors on the thermal conductivity measurement. However, in practice the resistance at the interface may be significantly smaller than 0.01 m^2 K/W so that the heat transfer problem is not influenced by the non-perfect thermal contact. We check this assumption by making several temperature measurements with different mechanical strength applied to the EPS foam slabs sandwiching the plane in order to vary the thermal contact resistance. Experimental results show that it has almost no influence on the temperature rise and thus, that the real thermal contact resistance is actually too small to disturb the transient heat transfer. Then, in all calculations, the thermal contact resistance between the plane and the surrounding medium will be neglected.

The comparisons of theoretical and experimental results concerning the evolution of the thermal conductivity estimated using the three different wires are illustrated on Figs. 3–6 for the four samples available. For clarity purpose, we

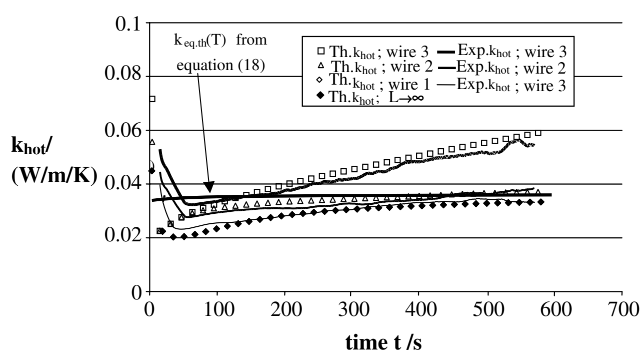

Fig. 3. Comparison of the estimated conductivity k_{hot} of sample no. 4 obtained experimentally and theoretically using the different hot-wires.

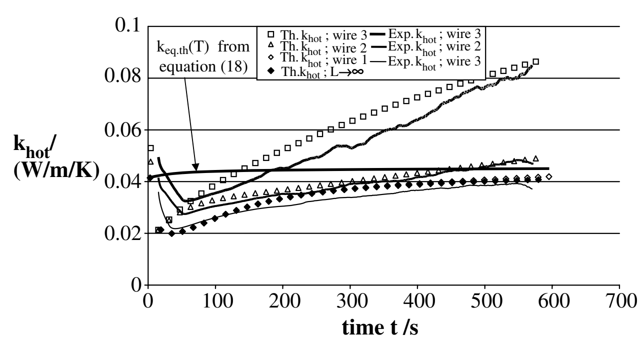

Fig. 4. Comparison of the estimated conductivity k_{hot} of sample no. 3 obtained experimentally and theoretically using the different hot-wires.

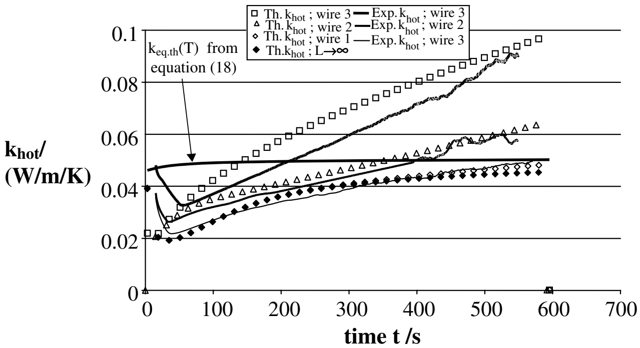

Fig. 5. Comparison of the estimated conductivity k_{hot} of sample no. 2 obtained experimentally and theoretically using the different hot-wires.

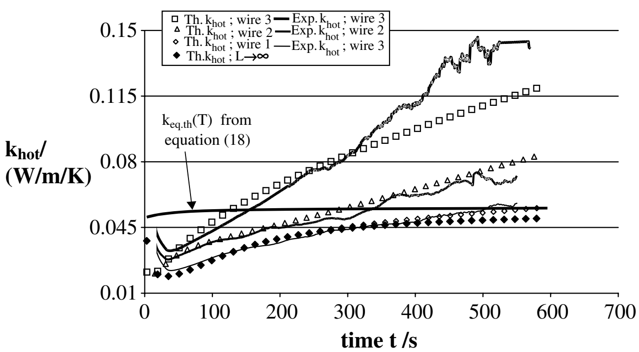

Fig. 6. Comparison of the estimated conductivity k_{hot} of sample no. 1 obtained experimentally and theoretically using the different hot-wires.

have not depicted the theoretical (th.) and experimental (exp.) temperature rise as they are close to each other for every foam samples and does not give interesting information on the hot-wire method. For each foam sample, we also carried out the calculations assuming an infinitely long wire ($L \to \infty$) with the same thermophysical properties as wire 1. Finally, we also show on each figure the evolution of the theoretical equivalent conductivity $k_{eq.th}(T)$ (Eq. (18)) obtained from the guarded hot-plate method. The results depicted were obtained using a heating power $\dot{Q} = 1.037$ W/m.

Concerning the evolution of the thermal conductivity k_{hot} estimated from Eq. (17), the agreement between theoretical and experimental results proves to be satisfactory whatever the foam sample and hot-wire used. Nevertheless, we notice that the theoretical prediction tends to slightly over-estimate the measured conductivity k_{hot}. This is not surprising and may be due to the fact that the radiative properties used slightly over estimate the radiative heat transfer as shown on Table 1, where we can notice that the predicted conductivities $k_{eq.th}$ are a little more important than the measured ones.

Both theoretical and experimental results show that the evolution of the estimated conductivity k_{hot} is strongly dependent on the hot-wire used. Indeed, when using wire 2 or 3, we observe, for all foam samples, a monotone and rapid increase of the estimated conductivity k_{hot} which rapidly exceeds the theoretical equivalent conductivity $k_{eq.th}$ stemming from the guarded hot-plate measurement. This increase of K_{hot} is faster for wire 3 with $L = 0.05$ m than for wire 2 ($L = 0.1$ m). When wire 1 ($L = 0.2$ m) is used, we also remark an increase of k_{hot} but it is noticeably slower. Moreover, when using wire 1, the estimated conductivity k_{hot} never exceeds $k_{eq.th}$ even when t reaches large values ($t \to 600$ s). The rate of increase of k_{hot} with t is well-predicted by the numerical simulation for every wire and whatever the foam sample used. However, the increase of k_{hot} with t observed for wire 2 and 3 is too fast to be only imputed to the small increase of the effective thermal conductivity of the foam $k_{eq.th}$ with the temperature (see Eq. (18)). At this stage, this is not possible to determine whether this increase is due to radiative phenomena or to limitations regarding the measuring apparatus.

In order to better understand the results observed, a more complete analysis of the influence of the different parameters has to be conducted. The influence of certain parameter, especially those related to the properties of foams used or to the measuring system, could not be varied and thus their influence could not be investigated experimentally. Our numerical simulation would then be a very useful tool to analyse their theoretical influence.

4.3.1. Influence of the wire length/Edge effects

The hot-wire apparatus must be compact in order to make measurements on relatively small samples. That is the reason why the usual length L of the heated wire is limited. At present, the longest wires available in the shops are 0.1 m in length. In classical hot-wire measurement on purely conductive materials, it is usually assumed that the wire is long enough to consider that the heat transfer remains one dimensional during the measurement duration and that edge effects can be neglected. The analysis of the results of Figs. 3–6 clearly shows that this assumption is no more valid when measurements are made on low-density thermal insulators. Indeed, as can be observed on the four figures, noticeable differences are found between the evolutions of k_{hot} estimated using the different apparatus. For the small time t, the difference observed between the results of the apparatus 2–3 ($L = 0.05$ m – $L = 0.1$ m) and the apparatus 1 ($L = 0.2$ m) are mainly due to the inertia effects. They are more important for the latter apparatus. On the other hand, for large time t, the inertia effect becomes negligible and the differences observed indicate that the assumption of one dimensional heat transfer is wrong when using standard hot-wire apparatus with $L \leqslant 0.1$ m on this kind of porous materials. Indeed, the length L has a strong influence on the heat transfer even for wire as long as 0.1 m.

Edge effects are characterized by an abnormal increase of the estimated conductivity k_{hot} with t. This increase is much faster than that of the effective thermal conductivity of the foam $k_{eq.th}$ with the temperature due to the radiative phenomenon (see Eq. (18)). The influence of edge effects is significant even for relatively small time t. For example, the theoretical results indicate that, for sample no. 3, the relative difference between k_{hot} calculated with $L = 0.05$ m and $L \to \infty$ (thermal inertia of wire 2–3) exceeds 5% as soon as t is greater than 70 s and reaches 50% at $t = 600$ s. The differences observed experimentally between the results obtained for $L = 0.05$ m and $L = 0.1$ m are of the same order of magnitude. When $L = 0.1$ m, the edge effects are less important but still significant and the rate of increase of k_{hot} is slower. As it was previously noted, from a certain measurement time t, the estimated thermal conductivity k_{hot} exceeds noticeably the equivalent thermal conductivity $k_{eq.th}$ measured by the guarded hot plate method. These observations clearly show that the classical hot-wire measuring method ($L \leqslant 0.1$ m) applied to such low-density insulating materials does not permit to determine a satisfactory equivalent thermal conductivity as the thermal conductivity k_{hot} estimated by the classical hot-wire method does not converge to a constant value but shows a continuous increase with the measurement time t. Then, two measurements made at different time t will lead to different value of the thermal conductivity.

Moreover, it appears experimentally and theoretically that a wire with $L = 0.2$ m is sufficient to avoid edge effects during all the measurement time ($t \leqslant 600$ s) for sample nos. 3 and 4. Indeed, the theoretical evolution of k_{hot} are almost identical when $L = 0.2$ m and $L \to \infty$ (thermal inertia of wire 1) for sample no. 4 whereas for sample no. 3, a very slight difference is observed when t reaches large values ($t > 500$ s). The relative differences between $L = 0.2$ m and $L \to \infty$ in both cases are respectively 0.2% and 2% at $t = 600$ s. On the other hand, for samples nos. 1 and 2, edge effects are still significant even when measurements are made using wire 1. Indeed, the relative differences between k_{hot} for $L = 0.2$ m and k_{hot} for $L \to \infty$ at $t = 600$ s are then 6.3% and 11%.

Theoretical and experimental results show that the influence of edge effects are more pronounced when measurements are made on materials with very low-density as the increase of k_{hot} with measurement time t is, then, faster than for heavier foams. This remark is valid whatever the length of the wire. In order to investigate more rigorously the influence of the density of the material, we carried out numerical simulations of the temperature rise for fictitious materials whose density varies from 10 kg/m^3 to 100 kg/m^3 using the hot-wire apparatus with different length $L = 0.05$ m, 0.1 m, 0.2 m and $L \to \infty$. The other properties of these materials are those of sample no. 3 presented in Section 4.1 and remain constant so that we only investigate the influence of the density. The results are illustrated on Table 3 where we show the evolution (according to ρ) of the relative differences between the estimated conductivity k_{hot} at $t = 600$ s obtained for a finite length ($L = 0.05$ m, $L = 0.1$ m or $L = 0.2$ m) and assuming an infinite wire, for the fictitious materials previously described.

This theoretical results confirm that when using standard hot-wire apparatus ($L = 0.05$ m or 0.1 m), edge effects may be significant even for materials with density beyond 50 kg/m^3. The classical hot-wire method is then poorly adapted to materials with low-density. On the contrary, when the length of the wire is 0.2 m, edge effects are almost negligible as long as the density of the material is greater than approximately 15 kg/m^3. For porous materials with lower densities, a longer wire is required to avoid edge effects.

Table 3
Theoretical variation of the relative error, due to edge effects, made on the conductivity K_{hot} estimated at $t = 600$ s for the fictitious materials

Length, L (m)	ρ (kg/m^3)				
	10	18.3	25	50	100
0.05	205%	131%	102%	52.3%	22%
0.1	67%	31%	19.2%	4.7%	0.7%
0.2	9%	2.3%	0.9%	0.1%	0.02%
∞	0%	0%	0%	0%	0%

4.3.2. Influence of the inertia of the wire

As was explained in Section 2.1, the thermal inertia of the wire per unit length ($\rho_w \cdot C_w \cdot \pi \cdot R_w^2$ in J/m/K) must be negligible in order for the hot-wire method to be rigorously applicable. In practice, the wires used have a certain inertia, as was observed in the previous paragraph when we compared the evolution of k_{hot} using different apparatus (1 and 2–3) at the small time t. However, inertia effects are especially significant at the beginning of the heating (small time t) when the temperature of the wire increases rapidly. When the time t is sufficiently important, the temperature rise gets slower and the proportion of energy used to heat the wire becomes negligible so that Eq. (2) could be used without causing errors. The heating duration t necessary for the inertia effects to be negligible is related to the inertia of the wire and to the inertia of the porous medium ($\rho \cdot C_p$) as well. In order to estimate this time t, we carried out the calculations of the temperature rise in sample no. 3 using fictitious wires of length $L = 0.2$ m and with different thermal inertia per unit length ($\rho_w \cdot C_w \cdot \pi \cdot R_w^2$).

The theoretical results indicate that, for measurements on low-density EPS foams, wires with relatively small inertia have to be used. Indeed, we notice that when measurements are made using a wire with a thermal inertia close to that of the wire 1 ($\rho_w \cdot C_w \cdot \pi \cdot R_w^2 = 1.62$ J/m/K), a measurement time $t = 600$ s is not sufficient for the inertia effects to be negligible. The theoretical error caused by inertia effects is then approximately 9%. The wire 1 is then not really adapted for the measurement of the thermal conductivity of low-density thermal insulators. On the other hand, if we used a hot-wire with the same thermal inertia per unit length as wires 2–3 ($\rho_w \cdot C_w \cdot \pi \cdot R_w^2 = 0.42$ J/m/K), the error would be only 2.5%.

We also investigated the influence of the inertia of the porous medium on the evolution of the error caused by inertia effect by carrying out the numerical simulation for the three other foams using the previous fictitious wires.

Table 4
Theoretical relative error, due to inertia effects, made on the conductivity k_{hot} estimated at $t = 600$ s using wire 1 or wire 2–3 with $L = 0.2$ m for each foam sample

Thermal inertia of the wire (J/m/K)	Sample number			
	1 ($\rho = 10$ kg/m^3)	2 ($\rho = 12.6$ kg/m^3)	3 ($\rho = 18.3$ kg/m^3)	4 ($\rho = 32$ kg/m^3)
$\rho_w \cdot C_w \cdot \pi \cdot R_w^2 = 1.62$ (wire 1)	11.3%	10.5%	9.8%	8.7%
$\rho_w \cdot C_w \cdot \pi \cdot R_w^2 = 0.42$ (wire 2–3)	3.9%	3.7%	3.5%	3.2%
$\rho_w \cdot C_w \cdot \pi \cdot R_w^2 = 0.0$	0%	0%	0%	0%

The results are illustrated on the Table 4 where we show the relative error made at $t = 600$ s when using wire 1 ($\rho_w \cdot C_w \cdot \pi \cdot R_w^2 = 1.62$ J/m/K, $L = 0.2$ m) or a wire with length $L = 0.2$ m having the same thermal inertia as wire 2–3 ($\rho_w \cdot C_w \cdot \pi \cdot R_w^2 = 0.42$ J/m/K).

As can be noticed, the relative error due to inertia effect varies slightly with the inertia of the porous medium. Indeed, the theoretical error on the estimation of k_{hot} at $t = 600$ s is always close to 10% for a wire with the same inertia as wire 1 and to 3–4% for wire 2–3. Nevertheless, we remark that the errors are a bit smaller when the hot-wire method is applied to relatively dense foams.

As a conclusion wire 1 doesn't prove to be not really adapted to the measurement on low-density EPS foams as its inertia is too important. On the other hand, if wire 2 and wire 3 were sufficiently long to neglect edge effects, they would be well adapted for the measurements on such media.

4.3.3. Influence of the heating power $\dot{Q}$

We investigated experimentally and theoretically the influence of the heating power on the hot-wire measurement by measuring and calculating the temperature rise for two other values of $\dot{Q}$: $\dot{Q} = 0.75$ W/m and $\dot{Q} = 1.5$ W/m. The theoretical and experimental results regarding the evolution of the estimated thermal conductivity k_{hot} of the sample no. 3 are illustrated on Fig. 7 for the three power used and for a length $L = 0.2$ m. We also carried out the same numerical simulations for an infinite wire and the results are depicted on this figure.

As can be seen, the power used for the heating of the wire has a slight influence on the estimated thermal conductivity. The evolutions are almost identical whatever the heating power used. However, it appears both experimentally and theoretically that a high heating power tends to increase k_{hot}. For example, when the power supplied is $\dot{Q} = 1.5$ W/m and the measurement time is 300 s, the predicted conductivity k_{hot} is approximately 2 mW/m/K higher than when $\dot{Q} = 0.75$ W/m. This difference is nearly the same for a finite wire ($L = 0.2$ m) or an infinite wire. For experimental results, the difference is difficult to estimate as the measured values fluctuate but it is the same order of magnitude and the agreement with the numerical simulation proves to be satisfactory again.

The slight influence of $\dot{Q}$ could be explained by the fact that when the heating power gets larger, the temperature reached near the wire is higher and the radiative energy emitted by the wire and the porous medium near the wire (which varies like T^4) is more important. The total heat transferred from the wire to the surrounding medium is then also more important and all is going on as if the conductivity k_c of the surrounding material was higher.

However, one can retain that the influence of $\dot{Q}$ remains relatively low.

4.3.4. Influence of radiative heat transfer on hot-wire measurement

In the previous paragraphs, the comparison between experimental and theoretical results has shown that the model developed provides satisfactory simulations of the temperature rise near the wire. Thus, we could use it to investigate theoretically the influence of the radiative contribution on the classical measurement of the estimated thermal conductivity k_{hot}. To do that, we carried out the theoretical calculations for four fictitious purely conductive materials (nos. 1′, 2′, 3′ and 4′) having the same theoretical equivalent conductivity $k_{eq.th}(T)$ (see Eq. (18)) and the same thermophysical properties ρ and C_p as the foams previously studied. The calculations are made using sufficiently long and thin wires to avoid inertia and edge effects. We used the following fictitious wires:

- $L = 0.2$ m for sample nos. 3 and 4.
- $L = 0.3$ m for sample nos. 1 and 2.

The other characteristics of the wires (R_w, $\rho_w \cdot C_w$, k_w and ε_w) are those of apparatuses 2–3 (see Table 2).

Then, we compared the evolutions of the temperature and of the estimated conductivity k_{hot} obtained for samples

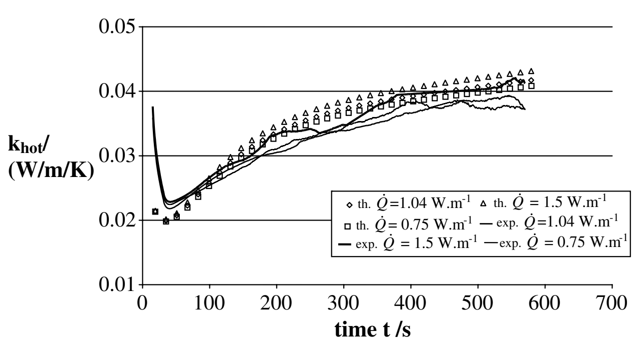

Fig. 7. Evolution of the theoretical and experimental thermal conductivity K_{hot} measured with wire 1 for sample no. 3 and different heating powers.

1′, 2′, 3′ and 4′ with those calculated for the four corresponding EPS samples. The thermal conductivity k_c of the fictitious materials nos. 1′, 2′, 3′ and 4′ are equal to the equivalent conductivity of sample nos. 1, 2, 3, 4:

$$k_c(T) = b_1 \cdot T^2 + b_2 \cdot T + b_3$$

where b_1, b_2 and b_3 are given in Table 1 for the foam sample nos. 1, 2, 3 and 4.

In the numerical model, as the radiative contribution is assumed null, we set $\vec{q}^{\,t}_{r_{i,j}} = \vec{0}$ and $(\nabla\vec{q}_r)^t_{i,j} = 0\ \forall t$, i and j. The numerical parameter used for the calculations are $nR = 12$; $nZ = 30$; S_6 quadrature; $Z_{\max} = 0.3$ m and $R_{\max} = 0.15$ m for samples nos. 3, 3′, 4 and 4′ ($L = 0.2$ m) and $nR = 12$; $nZ = 40$; S_6 quadrature; $Z_{\max} = 0.4$ m and $R_{\max} = 0.15$ m for samples nos. 1, 1′, 2 and 2′ ($L = 0.3$ m).

The other parameters are $\dot{Q} = 1.037$ W/m; $TR_c = 0$ K/W; $T_{\text{init}} = 296$ K and the numerical parameter are those used in Section 4.3.1.

The evolution of the temperature at $r = 1$ mm and of k_{hot} for the fictitious purely conductive materials and the corresponding EPS foams are illustrated on the Fig. 8. We also show the variation of the equivalent conductivity $k_{\text{eq.th}}$ (T) that would be obtained from guarded hot-plate measurements for each foam.

The comparison of the results on Fig. 8 shows that, during the hot-wire measurement, there are notable differences between the behaviour of purely conductive materials and materials where radiative heat transfer is significant even when the two materials have the same equivalent thermal conductivity and the same thermophysical properties.

Regarding the evolution of the temperature, one can notice that for a given heating power, the temperature near the wire reaches lower values when the surrounding medium is purely conductive than when there is a radiation/conduction coupling. The difference is more important for the very light foams in which the radiative contribution is more important. For samples nos. 1 and 1′ this difference reaches 2.8 K at $t = 600$ s whereas, it is almost negligible (<0.1 K) for samples nos. 4 and 4′. The very slight difference observed between the temperature rise for samples nos. 4 and 4′ could be explained by the fact that sample no. 4 is sufficiently opaque to be considered as optically thick. Then, the Rosseland approximation is valid and, although radiative transfer is not negligible in this sample, the total heat transfer follows a Fourier law. Then, all is going on as if the material was purely conductive with a conductivity $k = k_c + k_{\text{ROSS}}$ (Eq. (19)). On the other hand, when the optical thickness of the materials remains small the radiative transfer follows more complex laws and the thermal behaviour of the material differs from that of a purely conductive medium.

Concerning the evolution of the estimated conductivity k_{hot}, some important differences are also found when radiative heat transfer occurs especially for low time t. As for the temperature rise, these differences are more pronounced for the very light foams and are almost negligible for samples nos. 4 and 4′. We remark that, at the low time t (<200 s), when the influence of the inertia of the wire remains important, the theoretical k_{hot} obtained for the purely conductive materials is greater than for the corresponding EPS foam. Actually, the differences observed at low time t could be interpreted as an inertia effect due to

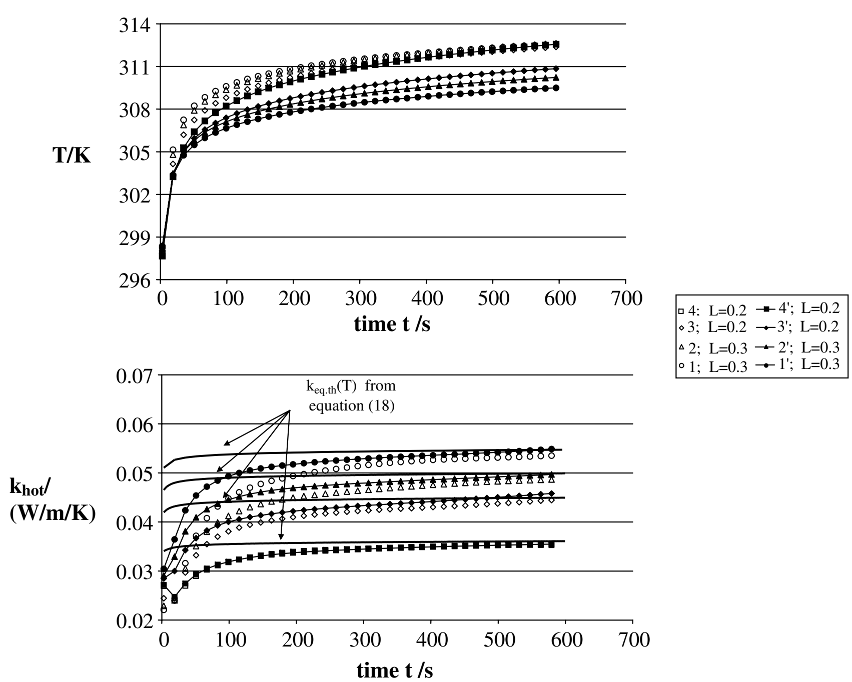

Fig. 8. Theoretical evolutions of the temperature and of the estimated conductivity k_{hot} for purely conductive materials nos. 1′, 2′, 3′, 4′ and the corresponding foam samples using an optimized wire.

the radiative heat transfer which is added to the inertia of the wire. This inertia effect is explained by the fundamentally different nature of the conductive heat transfer and radiative heat transfer in nearly transparent materials. However, one can observe that, as the measurement time reaches large values, the estimated conductivities k_{hot} of the foam samples tend to that computed for the corresponding purely conductive materials. At $t = 600$ s, the relative differences between the conductivities k_{hot} estimated for the purely conductive materials and semi-transparent foams are respectively 2.1%, 2.3%, 2.6% and 0.6% for sample nos. 1, 2, 3 and 4. These differences are negligible and might be due to the fact that the temperatures near the wire are not exactly the same for the purely conductive materials than for the foams. One can also notice that when the inertia of the wire and the inertia due to radiative contribution becomes negligible, the estimated conductivity k_{hot} for the foams sample follows the evolution of the equivalent conductivity $k_{eq.th}$ with the temperature expressed by Eq. (18).

As a consequence, we can conclude that, if the estimation of k_{hot} is made at after a time t sufficiently important, the thermal conductivity estimated by the hot-wire method is in close agreement with the equivalent thermal conductivity $k_{eq.th}$ measured from a guarded hot-plate method. Thus, it appears from the theoretical results that the hot-wire method could be extended to media in which the radiation/conduction coupling occurs even when the Rosseland approximation is not valid. Moreover, in comparison with the guarded hot-plate method, it could theoretically give additional information on the semi-transparent medium as it permits to measure the evolution of the equivalent conductivity with the temperature by making measurements at different time t or with different heating powers. Thus, it could be a very interesting method for characterizing in a more detailed manner the heat transfer in the medium studied as the increase of the equivalent thermal conductivity with the temperature T is closely related to the importance of radiative transfer.

Furthermore, we remark that the low-limit value of the time t at which the measurement should be made depends on the foam considered and is more important for light foams in which radiative contribution is more important. As example, for foam no. 1 which constitutes the lightest EPS foam available, a time t of approximately 400 s may be required if we use a hot-wire apparatus with $L = 0.3$ having the thermophysical properties of wire 2–3. On the other hand, for sample no. 4, the measurement could be made as soon as the influence of the inertia of the wire becomes negligible.

The previous numerical calculations have been carried out assuming that the wire constituting the measurement apparatus was perfectly black ($\varepsilon_w = 1$). This parameter influences directly the radiant energy emitted by the wire and thus, could affect the radiative transfer problem. Moreover, it is difficult to determine it precisely as it is composed of different materials with variable optical properties. Thus, in order to analyse the influence of the emissivity of the wire on the hot-wire measurement, we made theoretical calculations for each foam assuming different emissivity comprised ranging from 1 to 0.

The results show that it actually has a weak influence on the evolution of the estimated conductivity k_{hot}. This influence is characterized by a slight translation of k_{hot} to lower values when the wire is less emissive whereas the shape of the evolution with time t remains the same as when $\varepsilon_w = 1$. This could be explained by the fact that the radiant energy emitted by the wire and thus the heat transferred by radiation is less important when the emissivity of the wire decreases. As expected, we also noticed that the theoretical influence is more pronounced for light foams in which radiative transfer is more important. The translations of k_{hot} observed between a purely emissive and a purely reflecting wire are respectively 2.4 mW/m/K (4.6%), 1.8 mW/m/K (3.7%), 1.15 mW/m/K (2.6%) and 0.3 mW/m/K (1%) for the sample nos. 1, 2, 3 and 4. These differences are relatively weak but not negligible in the case of very light foams. However, in practice, the wire used in classical measurement apparatus are made of strongly absorbing materials (kapton, constantan) and the equivalent emissivity of the wire is close to 1. Thus, we could assume without significant errors that the emissivity of the wire has almost no influence on the estimated conductivity.

5. Conclusions

The hot-wire method is a technique for measuring the equivalent thermal conductivity. It is generally used for measurements on opaque media. At present, no study has already been conducted to investigate the application of this measuring method to low-density porous materials where both conductive and radiative heat transfer occur. In this article, we studied theoretically and experimentally the use of this technique on low-density EPS foams.

The theoretical and experimental results shown in the previous paragraphs permitted us to evaluate the influence of parameters such as the density of the material, the length of the wire, the thermal inertia of the wire, the heating power $\dot{Q}$ or the thermal contact resistance on the evolution of the estimated thermal conductivity k_{hot} of the material. For each of these parameters, the experimental results are well predicted by the numerical model simulating the 2-D axisymmetric transient coupled heat transfer around the wire. Thus, it proves to be a useful tool to investigate theoretically the application of the hot-wire method to light porous materials in which conductive and radiative transfer occur simultaneously.

The experimental and theoretical investigations revealed that classical hot-wire apparatus are poorly adapted to k_{eq} measurements on thermal insulators whose density is lower than 50 kg/m^3. Indeed, the maximum length of classical hot-wires ($L = 0.1$ m) is, then, not sufficiently important to avoid edge effects. A minimum length of 0.2 m is required in order to make satisfactory measurements. Theoretical and experimental k_{eq} results also showed that for such materials the errors caused by the thermal inertia of the wire could be significant when using classical apparatuses with relatively important thermal inertia such as wire 1. Inertia effects may be significant even when the estimation of k_{hot} is made at $t = 600$ s. Nevertheless, relatively thin wires such as wire 2 or 3 might have a sufficiently small thermal inertia per unit length in order for the hot-wire measurement to give satisfactory results. Thus, relatively long ($L \geqslant 0.2$ m) and thin ($\rho_{\mathrm{w}} \cdot C_{\mathrm{w}} \cdot \pi \cdot R_{\mathrm{w}}^2 \leqslant 0.42$) wires are required for the hot-wire measurement on low-density thermal insulators.

Finally, we also investigated the influence of the radiative heat transfer on the measurement by comparing the thermal behaviour of the EPS foams to that of fictitious purely conductive materials having the same thermophysical properties and the same equivalent thermal conductivities. The theoretical results showed that when the foam is too transparent to behave as an optically thick material (Rosseland approximation) the temperature rise near the wire is noticeably different and reaches higher values than for the corresponding fictitious purely conductive material. The influence of radiative transfer on the evolution of the estimated conductivity k_{hot} is then comparable to that observed when the thermal inertia of the wire is increased. Nevertheless, once the thermal inertia of the wire and the "inertia effect" due to radiative transfer become negligible, we observe that the theoretical conductivity k_{hot} tends to the equivalent thermal conductivity $k_{\mathrm{eq.th}}$ stemming from the simulation of the guarded hot-plate method and follows the evolution of $k_{\mathrm{eq.th}}$ with the temperature. Then, if the estimation of k_{hot} is made at a time t sufficiently important, the result of the hot-wire method is in close agreement with the equivalent conductivity obtained from the guarded hot-plate measurement. As a consequence, providing that the hot-wire is sufficiently long and has a sufficiently small inertia, this measuring method could be extended to media in which both conductive and radiative transfers occur. Moreover, contrary to the guarded hot-plate method, it could give additional information on the evolution of the equivalent conductivity of the material with the temperature by estimating the value of k_{hot} at different time t.

References

[1] M. Lazard, S. André, D. Maillet, Diffusivity measurement of semi-transparent media: model of the coupled transient heat transfer and experiments on glass, silica glass and zinc selenide, Int. J. Heat Mass Transfer 47 (2004) 477–487.

[2] B. Ladevie, Mise au point de dispositifs de caractérisation thermophysique de matériaux ioslants solides ou pâteux. Extension aux fluids cisaillés, ENSAM Bordeaux, 1998.

[3] J.P. Laurent, Optimisation d'outils de mesure in situ des paramètres thermiques: Application au matériau TERRE, INPG Grenoble, 1986.

[4] A. Saito, J.E.S. Venart, Radiation effect with the transient line source measurement of fluid thermal conductivity, in: Proceedings of the 6th International Heat Transfer Conference, Washington DC, USA, 1978, pp. 79–84.

[5] A. Saito, Review of the transient line source technique, JSME 23 (183) (1980) 1459–1466.

[6] J. Menashe, W.A. Wakeham, Effect of absorption of radiation on thermal conductivity measurements by the transient hot-wire technique, Int. J. Heat Mass Transfer 25 (5) (1982) 661–673.

[7] H.P. Ebert, J. Fricke, Influence of radiation transport on hot-wire thermal conductivity measurement, High Temp. High Pressure 30 (1998) 655–669.

[8] U. Gross, L.-T.-S. Tran, Radiation effects on transient hot-wire measurements in absorbing and emitting porous media, Int. J. Heat Mass Transfer 47 (2004) 3279–3290.

[9] R. Coquard, D. Baillis, Modeling of heat transfer in low-density EPS foams, J. Heat Transfer 28 (6) (2006) 538–549.

[10] H.S. Carlslaw, J.C. Jaeger, Conduction of Heat in solids, second ed., Oxford University Press, Oxford, 1959.

[11] R. Siegel, J.R. Howell, Thermal Radiation heat Transfer, third ed., Hemisphere Publishing Corp., Washington DC, 1992.

[12] R. Viskanta, J. Lim, Transient cooling of a cylindrical glass gob, J. Quant. Spectrosc. Rad. Transfer 73 (2002) 3279–3290.

[13] B.G. Carlson, K.D. Lathrop, Transport theory – the method of discrete ordinates, in: H. Greenspan, C.N. Kelber, D. Okrent (Eds.), Computing Methods in Reactor Physics, Gordon and Breach, New-York, 1968, pp. 165–266.

[14] S. Jendoubi, H.S. Lee, T.-K. Kim, Discrete Ordinates Solution for Radiatively Participating Media in a Cylindrical Enclosure, J. Thermophys. Heat Transfer 7 (2) (1993) 213–219.

[15] J.R. Tsai, M.N. Ozisik, Radiation in cylindrical symmetry with anisotropic scattering and variable properties, Int. J. Heat Mass Transfer 33 (12) (1990) 2651–2658.